

Article

Effect of Clearance and Cavity Geometries on Leakage Performance of a Stepped Labyrinth Seal

Min Seok Hur ¹, Soo In Lee ², Seong Won Moon ¹, Tong Seop Kim ^{1,*}, Jae Su Kwak ², Dong Hyun Kim ³ and Il Young Jung ³ 

¹ Department of Mechanical Engineering, Inha University, 100 Inha-ro, Michuhol-Gu, Incheon 22212, Korea; 22191280@inha.edu (M.S.H.); 22161642@inha.edu (S.W.M.)

² School of Aerospace and Mechanical Engineering, Korea Aerospace University, 76 Hanggongdaehak-ro, Deogyang-gu, Goyang 10540, Korea; sooin0510@kau.ac.kr (S.I.L.); jskwak@kau.ac.kr (J.S.K.)

³ Hanwha Aerospace Co. Ltd., 1204 Changwon-daero, Seongsans-gu, Changwon 51542, Korea; donghyu1.kim@hanwha.com (D.H.K.); iyjung@hanwha.com (I.Y.J.)

* Correspondence: kts@inha.ac.kr

Received: 11 October 2020; Accepted: 17 November 2020; Published: 19 November 2020



Abstract: This study evaluated the leakage characteristics of a stepped labyrinth seal. Experiments and computational fluid dynamics (CFD) analysis were conducted for a wide range of pressure ratios and clearance sizes, and the effect of the clearance on the leakage characteristics was analyzed by determining the performance of the seal using a dimensionless parameter. It was observed from the analysis that the performance parameter of the seal decreases as the clearance size increases, but it tends to increase when the clearance size exceeds a certain value. In other words, it was revealed that there exists a specific clearance size (S_{\min}) which minimizes the performance parameter of the seal. To identify the cause of this tendency change, a flow analysis was conducted using CFD. It was confirmed that the leakage characteristics of the stepped seal are affected by the size of the cavity, which is the space between the teeth. Therefore, a parametric study was conducted on the design parameters related to the cavity size (tooth height and pitch). The results show that the performance parameter decreases as the tooth height and pitch decreases. Moreover, S_{\min} increases as the tooth height increases and the pitch decreases.

Keywords: clearance; flow function; gas turbine; leakage; pressure ratio; stepped labyrinth seal

1. Introduction

The power and efficiency of gas turbines are being improved to meet the demands of users, leading to increased operating pressures and temperatures. However, the increased operating pressure and temperature increases the leakage flow at the blade tip, which disturbs the main flow and decreases turbine efficiency. Labyrinth seals are devices used to prevent such leakages and have benefits such as relatively simple structures and durability at high temperatures. Among the various geometric parameters of labyrinth seals, the parameter having the most dominant impact on the seal performance is the clearance size. The clearance size varies depending on the operating conditions (rotational speed and degree of thermal expansion of the blades) of the gas turbine. If the clearance is too large, the stage efficiency of the turbine decreases, and flow instability increases. In contrast, if it is too small, mechanical losses, such as wear, occur, thereby affecting the blade life [1]. Therefore, accurate predictions of the leakage characteristics of labyrinth seals according to the clearance are required.

Labyrinth seals are manufactured in various shapes by varying the arrangement of teeth to increase pressure loss and thereby reduce leakage. The commonly used geometries include straight seals with

teeth arranged in a straight line on one side, stepped seals with teeth arranged in the form of steps, and staggered seals with teeth arranged in a staggered manner. Many studies involving experimental and numerical analyses have been conducted to understand the complex flow phenomenon inside labyrinth seals. The most basic research was conducted by Vermes [2]. He performed experiments using a labyrinth seal with the most basic configuration and developed an analytical model based on the experimental data. Stocker et al. [3,4] conducted an experimental study on various seal geometries. They also investigated the sealing characteristics of several seals, including honeycomb seals considering the design parameters. Witting et al. [5–7] conducted experimental studies on the leakage characteristics of the flow and on heat transfer, and they analyzed the influence of the scale of the experiment and the rotation effect on the results. Tipton et al. [8] summarized previous studies on leakage prediction and analyzed the effects of the main design parameters of seals on leakage. Research on the characteristics of labyrinth seals has been performed steadily with the development of experimental methods and performance prediction software programs based on existing data [9,10].

During the past couple of decades, studies comprehensively evaluating the flow characteristics inside labyrinth seals have increased owing to advancements in experimental techniques and numerical methods. Zimmermann et al. [11] analyzed the effects of various design parameters of straight/stepped seals on leakage and examined the changes in the leakage characteristics of the seals due to the wear of the tooth tip. Rhode et al. [12] researched labyrinth seals with added grooves and observed changes in the flow field inside the seals using the flow visualization technique. Schramm et al. [13,14] optimized the geometry of labyrinth seals and compared the leakage characteristics of honeycomb and solid land seals using computational fluid dynamics (CFD). Willenborg et al. [15] performed experiments in a wide range of Reynolds numbers and confirmed that the discharge coefficient depended only on the pressure ratio at high Reynolds numbers. Doğu et al. [16] analyzed the leakage characteristics of mushroom-shaped labyrinth seals using CFD and confirmed that more leakage occurred due to shape changes, caused by rubbing. Yan et al. [17,18] conducted experiments and CFD analysis considering not only mushroom-shaped wear, but also deformation of teeth by bending. In addition, they conducted research on the hole-patterned labyrinth seal that arranged the holes regularly in the casing instead of honeycomb cells.

In recent years, experimental and numerical studies have focused on stepped labyrinth seals, which are the most common types of seals used to prevent leakage at the turbine blade tip. Kim et al. [19–21] conducted an experimental study on the pressure ratio and clearance size for straight/stepped seals and analyzed the leakage characteristics using CFD. Kang et al. [22] conducted experimental and numerical studies on stepped labyrinth seals according to the number of teeth and clearance size. They also compared the leakage characteristics of solid and honeycomb seals and confirmed that solid seals exhibited better sealing performance. Zhang et al. [23] performed experiments using clearance sizes applied to actual engine blades to exclude the influence of the scale of the experiments on the results. They also numerically analyzed the influence of various design parameters of stepped labyrinth seals, such as the clearance size, step height, and the number of teeth.

According to several previous studies, the performance parameters of stepped labyrinth seals tend to decrease as the clearance size increases [19–24]. However, some studies have reported that this is not always true, and the performance parameters tend to increase again as the clearance size exceeds a certain value [25]. Nevertheless, these studies did not present comprehensive cause-and-effect analyses. Therefore, it is necessary to conduct basic research on the performance parameter according to the clearance size. In this regard, we conducted experiments and CFD analysis in this study to analyze the leakage characteristics of a stepped labyrinth seal, and the effect of the clearance size on leakage performance was analyzed thoroughly. The stepped seal geometry used at the tips of rotating blades in gas turbines was selected as the target and a diverging flow path in which the diameter increases in the flow direction was considered the leakage flow path as in real applications in the tip section of turbine blades. The minimum performance parameter was determined by observing the leakage characteristics according to the clearance

size. To explain the cause for tendency change in the performance parameter, the effects of several design parameters (tooth height and pitch) on leakage were analyzed.

2. Labyrinth Seal and Experiment

2.1. Test Rig

Labyrinth seals used in actual gas turbines are ring-shaped, and there is an empty space (i.e., clearance or gap) between the rotating and stationary parts. However, it has been widely accepted that the rotation effect on the leakage flow rate is important only when the rotational speed is very high [7] and thus a stationary two-dimensional (2D) rig provides almost the same results as those obtained using an axisymmetric three-dimensional (3D) rig [4]. Therefore, numerous studies including those surveyed in the introduction have used 2D test rigs and 2D CFD simulations to obtain fundamental flow physics and accumulate vast amounts of information. Accordingly, a 2D test rig was also used in our study.

Figure 1 shows the overall configuration of the test rig and Figure 2 illustrates the geometry of the labyrinth seal used in the test. To minimize the 3D flow effect due to the wall, the width of the test section, which is the depth of the test section into the page of Figure 2, was set to be sufficiently large (approximately 67 times the smallest clearance size) compared to the clearance size. The components of the test rig included the air tank, valve, mass flow meter, honeycomb panel, and the test section. The pressure of the air inside the tank was as high as 8.5 bar and the pressure ratio was adjusted from 1.1 to 3.0 using the control valve between the tank and the test section. The pressure ratio (PR) was defined as the ratio of total pressure at the inlet to static pressure at the outlet of the test section. The inlet pressure was measured using a pressure transducer (PX409-050GI, OMEGA, Norwalk, CT, USA). The flow rate at each PR was measured using a thermal electronic mass flow meter (KMSG-8040MT, KOMETER, Incheon, Republic of Korea), and the inlet temperature was measured using a thermocouple (T-type SCPSS-040E-6, OMEGA, Norwalk, CT, USA). In addition, a honeycomb panel was installed at the inlet of the test section for ensuring straight and uniform flow, and the test section was scaled up to the actual geometry to improve the accuracy of the test results.

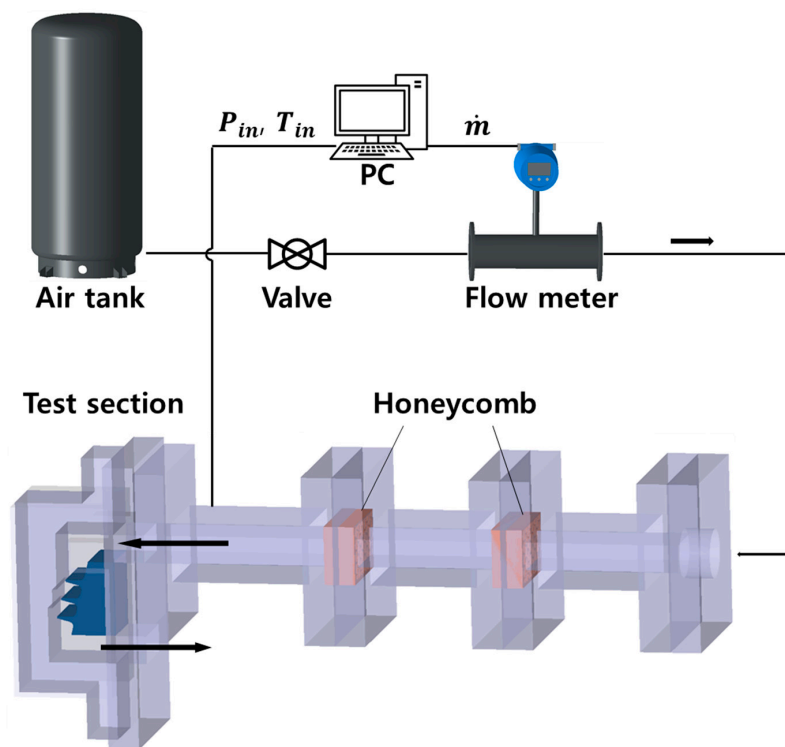


Figure 1. Schematic diagram of the test facility.

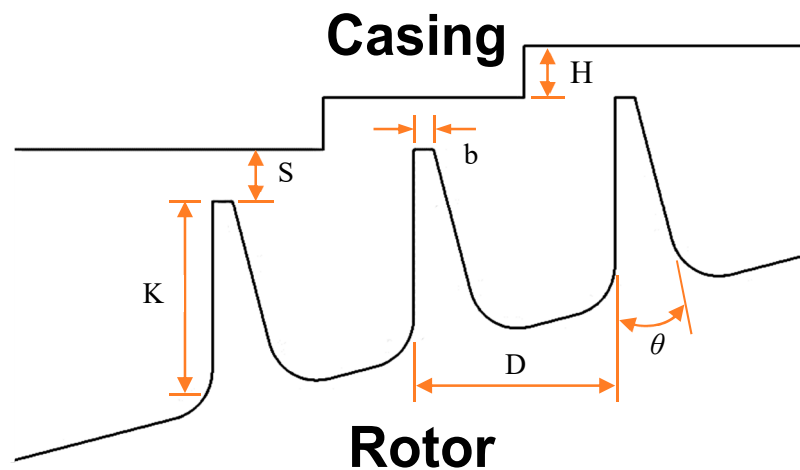


Figure 2. Seal geometry and parameters.

Table 1 summarizes the symbols and names of each design parameter and the non-dimensionalized expressions of the parameters of the labyrinth seal geometry. The test section was divided into an upper part and a lower part, which represent the stationary and rotating parts, respectively, in an actual turbine. The air comes into the test section from the left-hand side of Figure 2 and exits at the right-hand side, simulating a diverging flow path in actual turbine tip sections. The main geometric parameters of the stepped labyrinth seal include the clearance size (S), tooth thickness (b), tooth height (K), pitch (D), step height (H), and tooth angle (θ). In this study, numerical analysis and experiments were conducted by setting the range of the non-dimensionalized clearance size (step height ratio, S/H) from 0.2 to 1.2.

Table 1. Design parameters of the stepped labyrinth seal.

Parameter	Description	Value
S/H	Clearance/Step height	0.2~1.2
D/H	Pitch/Step height	4
K/H	Tooth height/Step height	4
θ	Tooth angle	15°
N	Number of teeth	3

2.2. Seal Performance

The performance of the labyrinth seal was determined using the relationship between the PR and a performance parameter. The most commonly used performance parameter is the flow function, which is defined in Equation (1).

$$\phi = \frac{\dot{m} \sqrt{T_{o,in}}}{A_C P_{o,in}} \quad (1)$$

where \dot{m} is the flow rate, A_C is the throat area, $P_{o,in}$ is the inlet total pressure, $T_{o,in}$ is the inlet total temperature. The flow function is the semi-dimensionless number which facilitates real leakage flow rate prediction for any arbitrary operating condition. The smaller the flow function is, the better the performance of the labyrinth seal becomes.

2.3. Measurement Uncertainty

The method proposed by Kline [26] was used to check the measurement uncertainty. The equation used for calculating the uncertainty of the flow function is given below.

$$\Delta\phi = \sqrt{\left(\frac{\partial\phi}{\partial\dot{m}}\Delta\dot{m}\right)^2 + \left(\frac{\partial\phi}{\partial T_0}\Delta T_0\right)^2 + \left(\frac{\partial\phi}{\partial S}\Delta S\right)^2 + \left(\frac{\partial\phi}{\partial d}\Delta d\right)^2 + \left(\frac{\partial\phi}{\partial P_0}\Delta P_0\right)^2} \quad (2)$$

$$u = \frac{\Delta\phi}{\phi} \quad (3)$$

We used 0.3% of the measured flow rate as the uncertainty of the mass flow rate measurement ($\Delta\dot{m}$) and 0.5 °C as that of the temperature (ΔT_0) according to the manufacturer's manual. The uncertainty of the tip clearance measurement (ΔS) was set at 0.01 mm according to the least count of the gap gauge, and the uncertainty of the section width measurement (Δd) was set at 0.005 mm according to the least count of the Vernier calipers. The sum of 0.01% of the maximum measurable limit and 0.008% of the measured value was used as the value for the uncertainty of the pressure measurement (ΔP_0) according to the manufacturer's manual. Therefore, the uncertainty of the flow function (u) was calculated to be 3.4%.

3. Analysis

3.1. Numerical Approach

ANSYS CFX (ver. 19.0, ANSYS Inc., Canonsburg, PA, USA, 2018) [27], a commercial software program, was used for CFD analysis. Figure 3 shows examples of the analysis domain and grid structure. As the 2D flow was secured in the experiment, the 2D calculations were also sufficient for CFD. However, as ANSYS CFX is based on 3D calculations, the 3D domain was set as shown in Figure 1; nevertheless, we ensured that the 3D was practically close to the 2D domain by setting the smallest width as far as we could and applied symmetry conditions to lateral faces. This method is recommended for 2D calculations according to the CFX manual [28]. ANSYS ICEM (ver. 19.0, ANSYS Inc., Canonsburg, PA, USA, 2018) was used for mesh generation. The grids of the overall leakage flow path were composed of unstructured meshes and only the wall portion was composed of prism layers so that y^+ could be ≤ 2 . Figure 3 shows an example of generated meshes. It is clearly shown that dense meshes were generated around the tip clearance. Grid dependence tests were performed to select appropriate numbers of meshes. Figure 4 illustrates an example for the case when the clearance to step height ratio (S/H) is 0.4. The results confirmed that the flow function, which was the target function, became almost constant when the number of meshes was 120,000 or more. Accordingly, 130,000 meshes were adopted in a specific case. Of course, the number of meshes generally increased as the clearance increased. It ranged from 130,000 to 150,000 when the S/H ratio increased from 0.2 to 1.2.

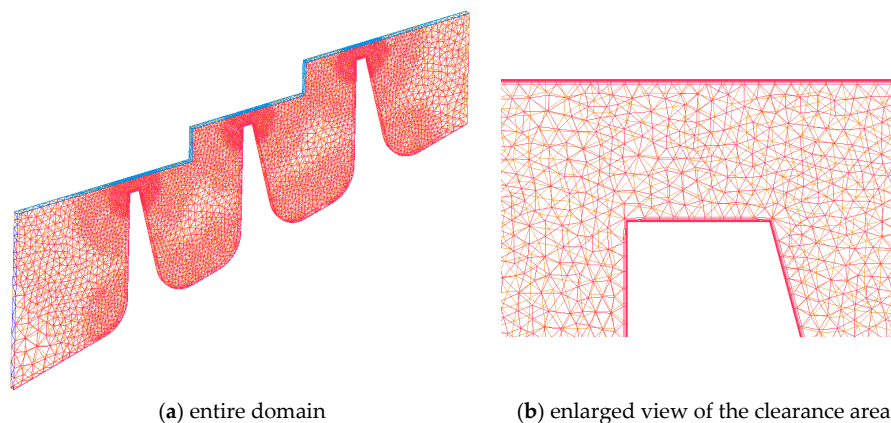


Figure 3. Example of the computational domain and meshes ($S/H = 0.4$).

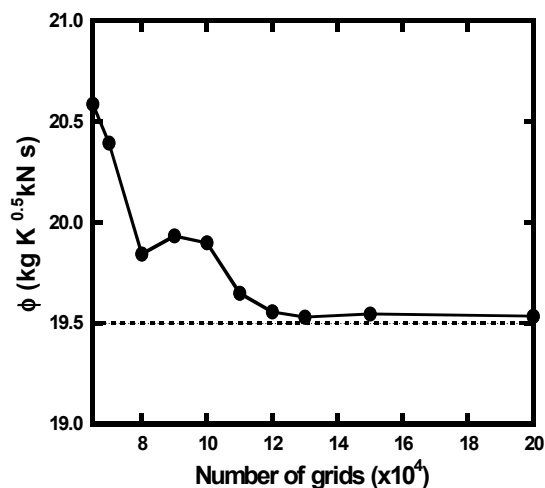


Figure 4. Example of grid dependence of the computational fluid dynamics (CFD) result ($S/H = 0.4$).

3.2. Boundary Conditions and Validation

Inlet total pressure and temperature and outlet static pressure were used as boundary conditions to simulate the operating conditions of the test. Adiabatic and no-slip conditions were used for the solid surfaces, and the symmetry condition was used at the two side boundary surfaces (lateral faces). The high-resolution advection scheme was used, which adequately uses the first and second order scheme depending on the situation, satisfying both the numerical stability and accuracy of the analysis. In addition, the first-order turbulence numerics was selected. The residual value (RMS) of the flow parameter was set to less than 1.0×10^{-4} as the convergence condition for the analyses. Table 2 summarizes the numerical analysis method and boundary conditions. A turbulence model that accurately captures the flow characteristics inside the seal cavity is required because of a strong vortex flow which is one of the major causes of the pressure loss in the seal. Therefore, the SST turbulence model, which is known to predict the vortex size and separation point accurately [29,30], was adopted. Figure 5 compares the sample test run results obtained using the SST model with those obtained using other turbulence models ($k-\omega$, $k-\epsilon$ and RNG $k-\epsilon$ models). Although there were no significant differences in the calculation results obtained using the various turbulence models, the SST model produced results closest to the experimental values with errors less than 3%. In addition, a comparison between the experimental and CFD results shown in Figure 6 confirms that CFD has sufficient accuracy for evaluating the leakage performance of the labyrinth seal.

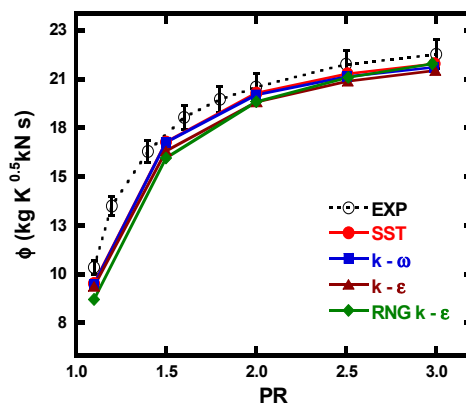


Figure 5. Comparison of turbulence models ($S/H = 1.0$, $K/H = 4$, $D/H = 4$).

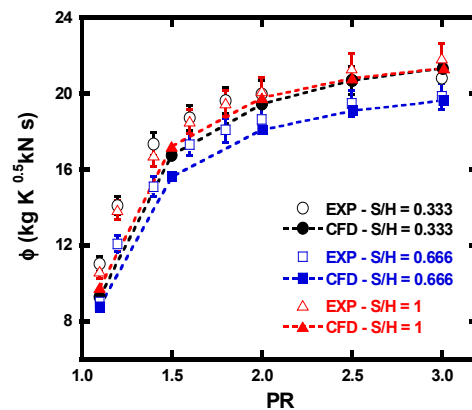


Figure 6. Comparison between the CFD and experimental results ($K/H = 4$, $D/H = 4$).

Table 2. Numerical methods and boundary conditions.

Software	ANSYS CFX 19.0
Turbulence model	Shear Stress Transport (SST)
Advection scheme	High resolution
Fluid	Air (ideal gas)
Pressure ratio	1.1~3.0
Inlet total temperature	295 K
Outlet static pressure	101.325 kPa
Wall	Adiabatic, no slip
Lateral faces	Symmetry

4. Results and Discussion

4.1. Leakage Characteristics According to Clearance Size

Figure 7 shows the flow function obtained using CFD at different PR and S/H values. For all S/H values, the flow function increases as the PR increases and exhibited choking after a certain PR. For example, the choking pressure ratio is around 2.5 when S/H is 0.2. As well known, the fact that the flow becomes choked does not necessarily mean that the actual flow rate is constant. It varies with the inlet total pressure and temperature. In our cases, the actual mass flow rate increases in proportion to the inlet total pressure because a higher pressure ratio means a higher inlet total pressure: remember that the inlet total temperature and the outlet static pressure were fixed.

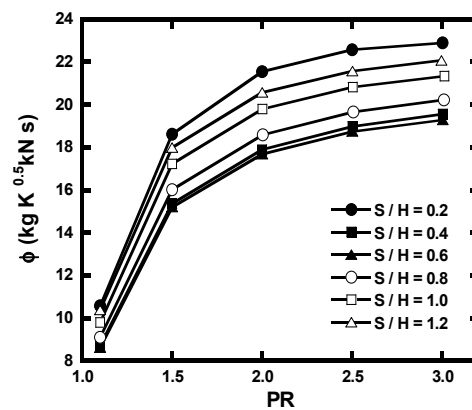


Figure 7. Variations in flow function with pressure ratio (PR) and S/H ($K/H = 4$, $D/H = 4$).

An important observation was that change in flow parameter due to the increase in the clearance size clearly differs below and above $S/H = 0.6$. To intensively examine changes in the flow function according to the clearance, the flow function at the PR of 2.5 was plotted in Figure 8 and compared with the experimental values under the same conditions. As the clearance increases, the flow function decreases and then tends to increase again at a certain clearance size, as observed commonly in the CFD and experimental results. This result confirmed that the stepped labyrinth seal has a specific clearance size (S_{\min}) that minimizes the flow function. It should be noted that the flow function does not represent the actual leakage flow rate but indicate relative leakage performance. Therefore, a lower flow function does not necessarily mean a lower flow rate but represents a better relative seal performance. The actual leakage flow rate increases as the clearance size increases in all the test cases in our study.

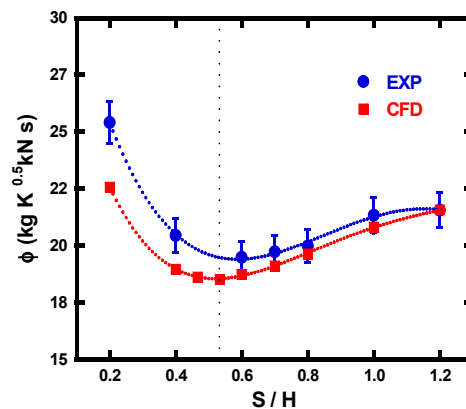


Figure 8. Variation in flow function with S/H (PR = 2.5, $K/H = 4$, $D/H = 4$).

To identify the cause of such changes in the flow function due to the increase in the clearance size, the flow inside the seal was analyzed using the details of the flow phenomena obtained by CFD. Figures 9 and 10 show the contours of the total pressure and static pressure, respectively, for various S/H ratios at the PR of 2.5. As S/H increases, the flow through the clearance develops a type of high-speed flow layer (see Figure 9). Figure 10 shows that the flow layer passing the clearance collides with the next tooth, resulting in a local increase in static pressure, which means that the kinetic energy of the leakage flow significantly dissipates. The collision point moves toward the tooth tip gradually as the S/H increases, and after $S/H = 1.0$, it is located at the tip of the tooth. In other words, in the specific S/H range in which the flow function decreased (S/H from 0.2 to 0.533), the flow rate gradually increases and the pressure loss due to collision with the tooth increases, improving the sealing performance. However, when the clearance continues to increase over the critical value of 0.533, most of the leakage flow through the previous clearance directs to the next clearance space without hitting the tooth, as shown in Figure 9. Accordingly, the kinetic energy loss caused by the collision reduced, resulting in a decrease in the sealing performance. In addition, it is seen from Figure 9 that the total pressure inside the cavity slightly increases as S/H increases from 0.2 to 0.533. This indicates that the leakage performance improves (i.e., the flow function decreases) as the flow trapped inside the cavity is increased by the flow layer moving at a high speed. However, after $S/H = 0.533$, the total pressure inside the cavity tends to decrease which means the flow trapped inside the cavity decreases. Figure 11 clarifies the change of the pressure inside the cavity with respect to S/H . It shows the variation in the averaged total pressure inside the cavity according to S/H , which clearly shows that total pressure decreases after the maximum point.

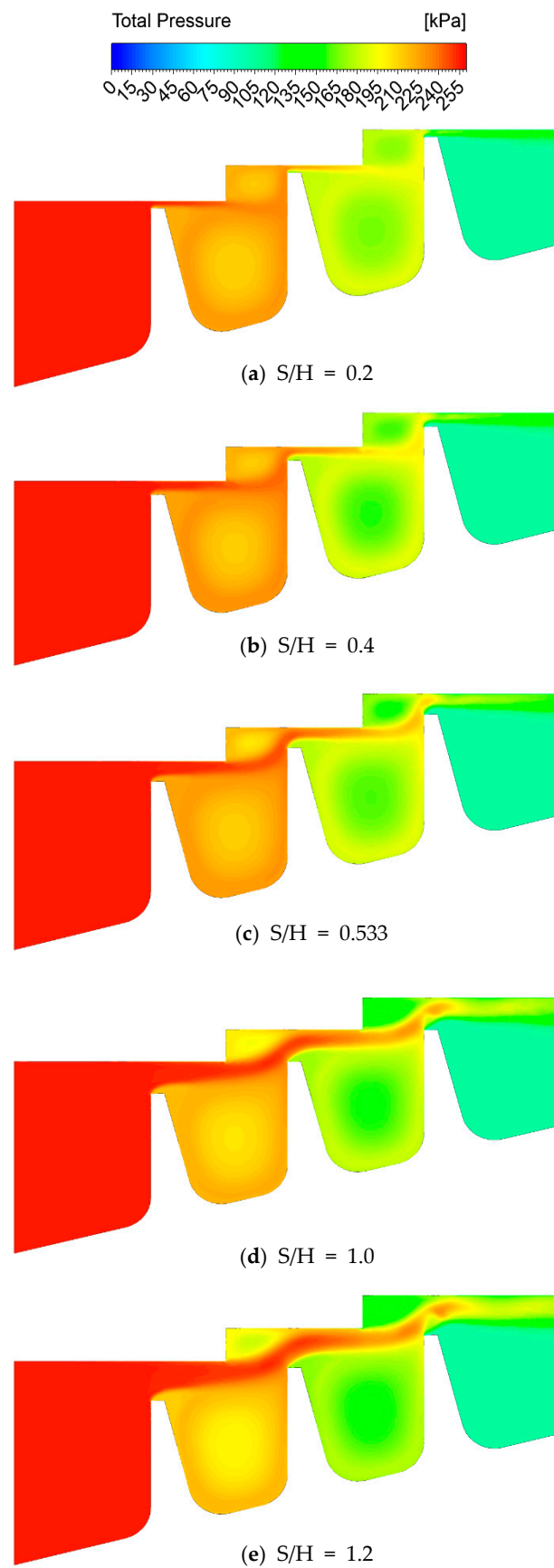


Figure 9. Total pressure contour plots for various S/H ratios (PR = 2.5, K/H = 4, D/H = 4).

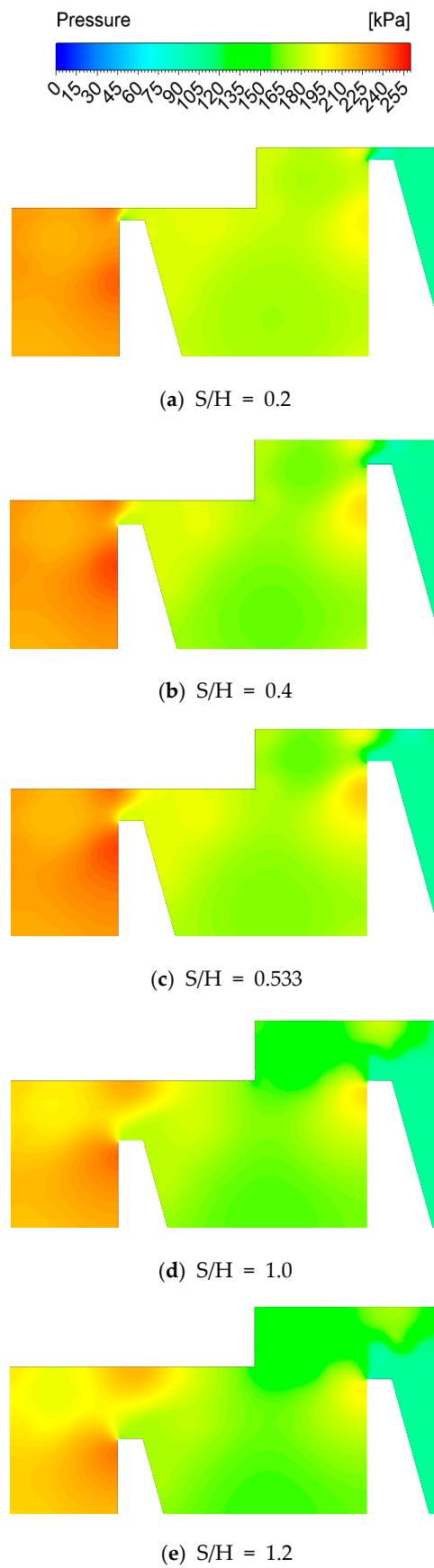


Figure 10. Static pressure contour plots for various S/H ratios ($PR = 2.5, K/H = 4, D/H = 4$).

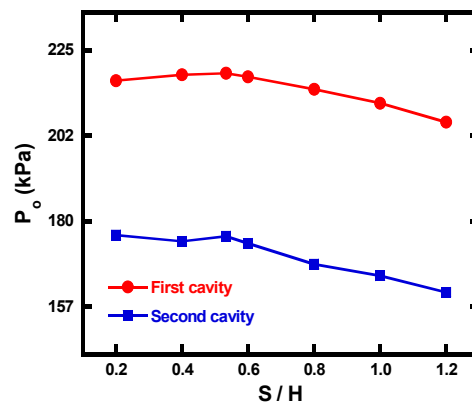


Figure 11. Variation in the averaged total pressure inside the cavity with S/H ($PR = 2.5$, $K/H = 4$, $D/H = 4$).

In summary, the tendency of the variations in flow function with clearance change at $S/H = 0.533$. In other words, when the clearance size is approximately half the step height, the maximum resistance to leakage flow occurs, leading to decreases in the flow function. As the clearance size further increases, the resistance to leakage flow decreases, leading to increases in the flow function.

4.2. Parametric Study on the Impact of Cavity Size

4.2.1. Outline

Through the flow analysis, we identified two main reasons for the reduced flow function (i.e., enhanced leakage performance) of the stepped labyrinth seal. The first is the significant dissipation of the kinetic energy during the leakage flow that occurs as the fluid passing through the clearance collides with the next tooth. The second is the formation of a strong flow layer owing to the high-speed flow passing through the clearance and the subsequent confinement of the rotating flow inside the cavity. The identification indicates that the leakage characteristics of the stepped labyrinth seal are affected not only by the clearance size but also by the value of S/H relative to the cavity size. Based on this observation, a parametric study on the tooth height and pitch, which are geometrical parameters affecting the cavity size, was conducted using the CFD. Table 3 gives the analysis range set for each parameter.

Table 3. Variation range of the non-dimensional parameters.

Parameter	Description	Value	Variation Range
D/H	Pitch/Step height	4	2~6
K/H	Tooth height/Step height	4	3~5

4.2.2. Tooth Height

Figure 12 shows the change in the flow function according to the values of S/H and K/H at the PR of 2.5. As the value of K/H decreases, the flow function decreases. The minimum value of the flow function is 8.4% lower at $K/H = 2$ and 5.9% higher at $K/H = 6$ compared to the reference value at $K/H = 4$. Figure 13 shows the velocity vector according to the K/H value at constant S/H and PR values. As the value of K/H decreases, the cavity size decreases, thereby increasing the velocity of the rotating flow in the cavity. Accordingly, a high-velocity flow layer is formed at the point where the flow in the axial direction (i.e., the throughflow) and the rotating flow inside the cavity joined. Following this, the joined flow collides with the tooth, increasing the local pressure, as shown in Figure 14. This indicates significant dissipation of the kinetic energy is induced by the leakage flow. In addition, as the velocity of the flow layer is higher, a larger separation occurs at the tooth tip, as shown in the velocity contour of Figure 15. This reduces the flow function because the effective area in which the flow can actually move is reduced. In addition, as the tooth height decreases, S_{\min} slowly decreases owing to the reduced flow rate inside the cavity.

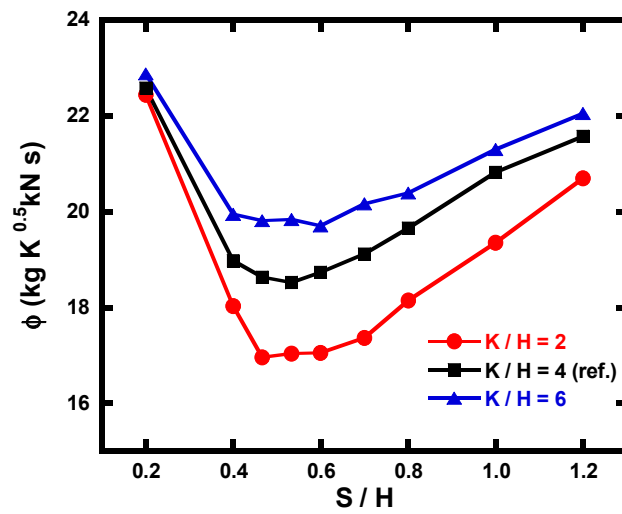


Figure 12. Variation in the flow function with S/H and K/H (PR = 2.5, D/H = 4).

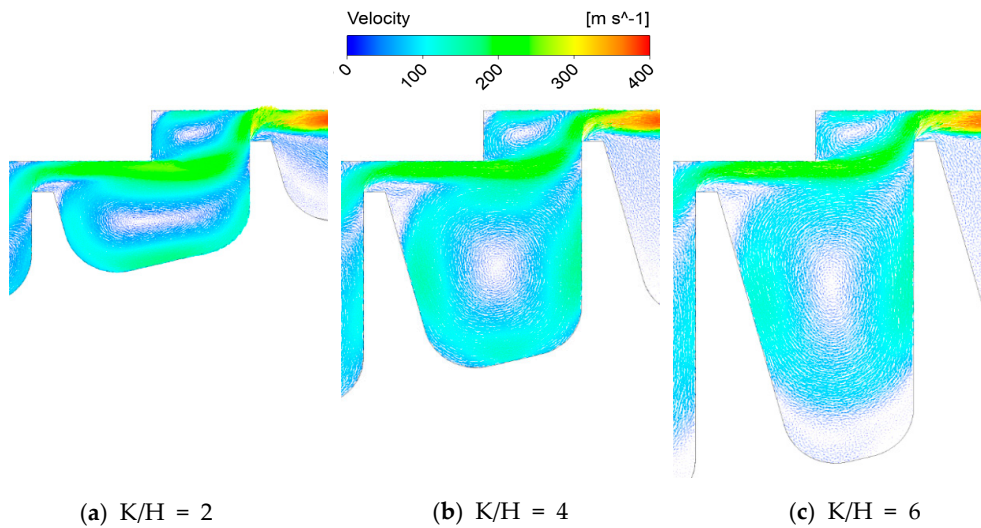


Figure 13. Velocity vectors for various K/H ratios (PR = 2.5, S/H = 0.6, D/H = 4).

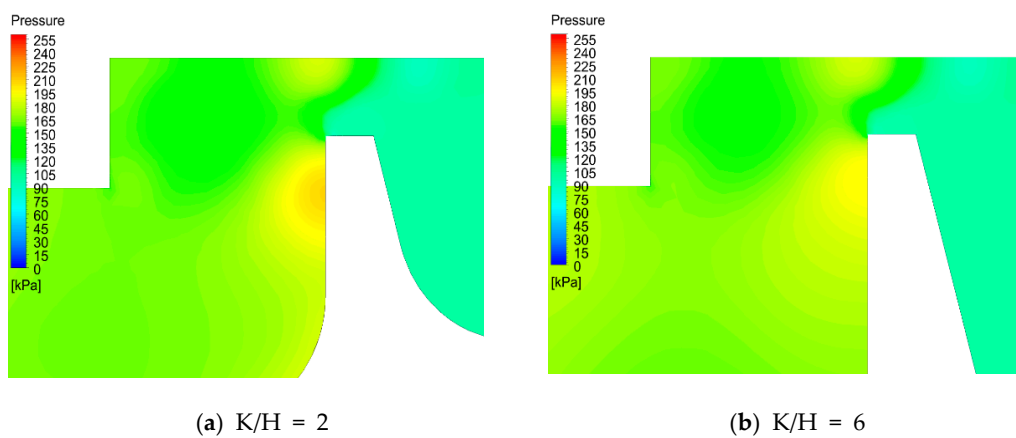


Figure 14. Static pressure contour plots for the smallest and largest K/H ratios (PR = 2.5, S/H = 0.6, D/H = 4).

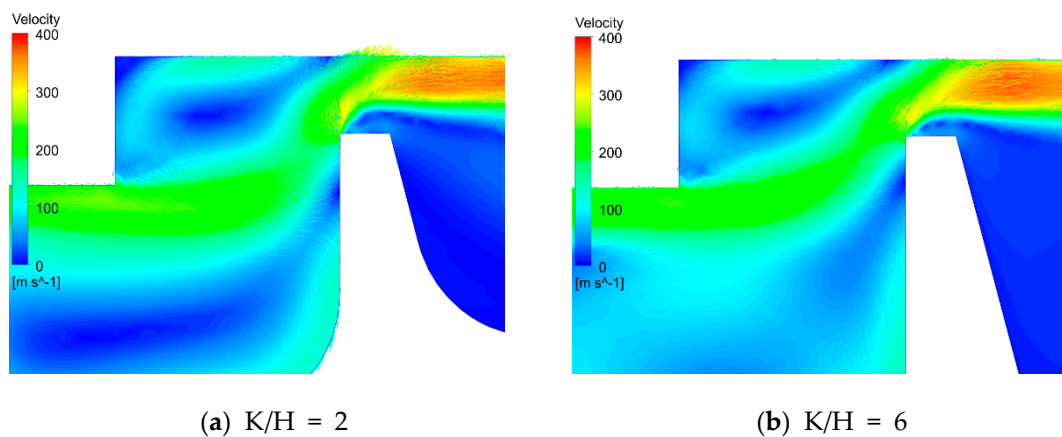


Figure 15. Velocity contour plots for the smallest and largest K/H ratios ($PR = 2.5$, $S/H = 0.6$, $D/H = 4$).

The impact of S/H is summarized as follows. At $S/H = 0.2$ which is the smallest value in our study, the change in tooth height did not affect the flow function (see Figure 12) because the clearance is too small for the flow separation to be an important factor. As S/H increases, the influence of K/H increases, which means the favorable impact of a lower K/H increases. However, as S/H increases above the minimum flow function point, the influence of K/H increases again.

4.2.3. Pitch

Figure 16 shows the flow function according to the S/H and D/H values at the PR of 2.5. As the value of D/H decreases, the flow function decreases. The minimum value of the flow function is 5.4 % lower at $D/H = 3$ and 0.7% higher at $D/H = 5$ compared to the reference value at $D/H = 4$. Figure 17 shows the streamlines when D/H is the highest and lowest at constant S/H and PR values. As D/H decreases, the velocity of the flow layer increases because the travel distance of the flow in the axial direction decreases. In addition, larger separation occurs because of the rapid movement of the flow in the radial direction. This reduces the effective area, thereby further increasing the leakage reduction effect (see Figure 18). In addition, as the pitch decreases, S_{\min} tends to increase. This is because flow into the cavity continuously occurs despite the increase in cavity size owing to the reduction in the travel distance in the axial direction.

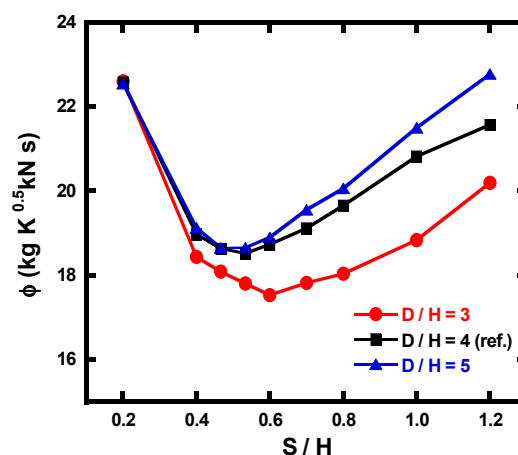


Figure 16. Variation in the flow function with S/H and D/H ($PR = 2.5$, $K/H = 4$).

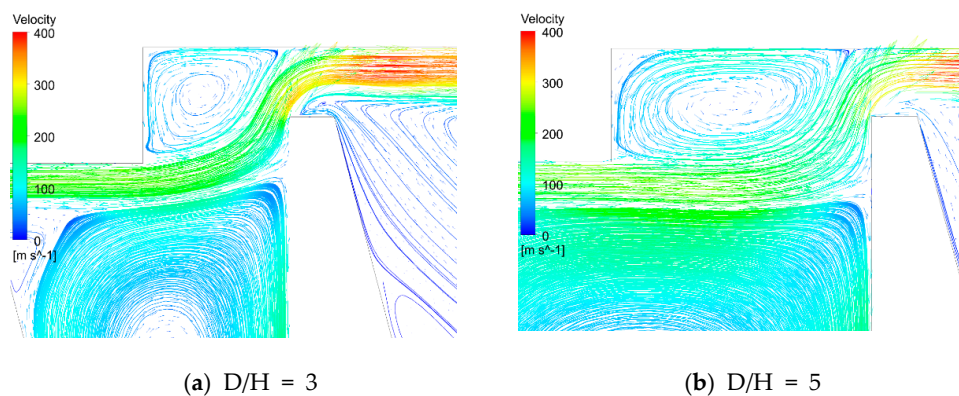


Figure 17. Velocity streamline plots for the smallest and largest D/H ratios ($PR = 2.5$, $S/H = 0.6$, $K/H = 4$).

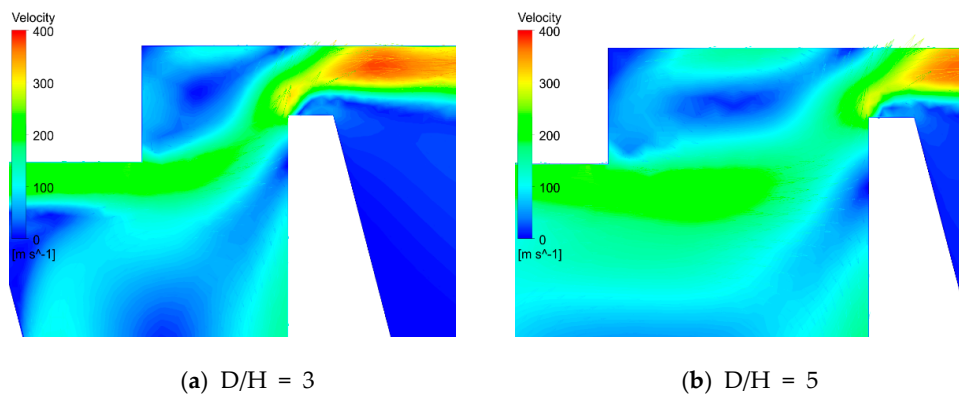


Figure 18. Velocity contour plots for the smallest and largest D/H ratios ($PR = 2.5$, $S/H = 0.6$, $K/H = 4$).

As with the case of the tooth height, when $S/H = 0.2$, the change in pitch does not affect the flow function because the clearance is too small for the flow separation to be an important factor. Despite the increase in the clearance size, changes in the flow function due to the pitch were hardly observed before S_{\min} . Although the relative flow velocity decreases owing to the increase in the travel distance in the axial direction, there is almost no difference in the overall leakage performance because the flow rate into the cavity increases. However, as the clearance continues to increase, the flow rate inside the cavity sharply decreases, causing differences in the flow function owing to the difference in the velocity of the flow layer.

4.2.4. Summary of the Parametric Study

The results obtained from analyzing the effects of the tooth height and pitch on leakage performance can be summarized as follows. Overall, changes in the tooth height cause more significant changes in leakage characteristics than changes in the pitch. The influence of the clearance change is also stronger according to the tooth height variation. In addition, when the clearance is considerably small, changes in the two design parameters have little influence on the flow function. However, as the clearance gradually increases, the flow function shows different tendencies owing to changes in the two design parameters before and after S_{\min} . As the values of both the parameters decrease, the leakage performance improves (i.e., the flow function decreases), but S_{\min} decreases as K/H decreases and D/H increases. As the tooth height decreases, S_{\min} decreases owing to the reduction in the flow rate into the cavity. In contrast, as the pitch decreases, the flow rate into the cavity decreases, but S_{\min} increases because the flow into the cavity continuously occurs despite the increase in the clearance size due to the relatively reduced travel distance in the axial direction.

5. Conclusions

In this study, the leakage characteristics of a stepped labyrinth seal, which is mainly used for sealing at the blade tips of gas turbines, were analyzed through experiments and CFD simulations for a wide range of PRs and clearance sizes. We focused on determining the clearance size at which the tendency of the flow function changed owing to changes in the design parameters. The main results and conclusions of this study are summarized as follows:

1. As the clearance size increases, the flow function of the seal decreases initially, but it tends to increase at a certain clearance size. In other words, the stepped labyrinth seal has a clearance size that minimizes the flow function and this specific clearance size is approximately half the step height ($S/H = 0.533$). This change in the tendency of the flow function was examined through flow analysis. The analysis results showed that the leakage characteristics of the stepped labyrinth seal are affected by the value of S/H relative to the cavity size.
2. The flow function of the stepped labyrinth seal is affected by the tooth height and pitch, and the leakage reduction effect increases as both these geometric parameters decrease (the minimum value of the flow function is 8.4% lower at $K/H = 2$ in comparison to the reference value at $K/H = 4$ and 5.4% lower at $D/H = 3$ in comparison to the reference value at $D/H = 4$). In addition, as the tooth height and pitch decrease, the changes in flow function due to the increase in clearance increase. When the clearance is considerably small, changes in the tooth height and pitch hardly affect the flow function.
3. The most important conclusion obtained in this study is that the stepped labyrinth seal has a specific clearance size (S_{\min}) at which the flow function is minimized. The finding that S_{\min} varies depending on the tooth height and pitch is also important. Another important finding is that S_{\min} decreases as the tooth height increases and the pitch decreases. This study is significant in that it provides basic data required for optimizing the geometry of stepped labyrinth seals to improve their leakage performance through determining the clearance size and geometric parameters that minimize the flow function.

Author Contributions: Conceptualization, M.S.H., T.S.K., methodology, M.S.H., S.I.L., S.W.M., software, M.S.H., S.W.M., validation, M.S.H., S.I.L., formal analysis, M.S.H., investigation, M.S.H., S.I.L., resources, T.S.K., J.S.K., data curation, M.S.H., writing—original draft, M.S.H., S.I.L., writing—review and editing, T.S.K., M.S.H., supervision, T.S.K., J.S.K., project administration, I.Y.J., D.H.K., and funding acquisition, T.S.K., J.S.K., I.Y.J., D.H.K. All authors have read and agreed to the published version of the manuscript.

Funding: This study was conducted with the support of the Korea Evaluation Institute of Industrial Technology (KEIT) at the Ministry of Industry, Commerce and Energy in 2020 (No. 20002700). The authors gratefully acknowledge this support.

Conflicts of Interest: The authors declare no conflict of interest.

Nomenclature

A_c	Throat area [m ²]
b	Tooth width [mm]
D	Pitch [mm]
d	Test section width [mm]
H	Step height [mm]
K	Tooth height [mm]
k	Specific heat ratio
\dot{m}	Mass flow rate [kg/s]
N	Number of teeth
P_o	Total pressure [kPa]
P	Static pressure [kPa]
PR	Pressure ratio
R	Gas constant [kJ/kg · K]
S	Clearance [mm]
S_{\min}	Clearance for a minimal flow function [mm]
T_o	Total temperature [K]
u	Uncertainty
ϕ	Flow function [kgK ^{0.5} /kNs]
θ	Tooth angle [°]

Subscripts

c	Contraction
in	Inlet
min	Minimum
out	Outlet

References

1. Lattime, S.B.; Steinetz, B.M. *Turbine Clearance Control Systems: Current Practices and Future Directions*; TM-2002-211794; NASA: Washington, DC, USA, 2002.
2. Vermes, G. A fluid mechanics approach to the labyrinth seal leakage problem. *J. Eng. Power* **1961**, *83*, 161–169. [[CrossRef](#)]
3. Stocker, H.L.; Cox, D.M.; Holle, G.F. *Aerodynamic Performance of Conventional and Advanced Design Labyrinth Seals with Solid-Smooth, Abradable, and Honeycomb Lands*; CR-135307; NASA: Washington, DC, USA, 1977.
4. Stocker, H.L. Determining and improving labyrinth seal performance in current and advanced high performance gas turbines. *AGARD Conf. Proc.* **1978**, *237*, 13.1–13.22.
5. Wittig, S.; Dorr, L.; Kim, S. Scaling effects on leakage losses in labyrinth seals. *J. Eng. Power* **1983**, *105*, 305–309. [[CrossRef](#)]
6. Wittig, S.; Schelling, U.; Jacobsen, K.; Kim, S. Numerical Predictions and Measurements of Discharge Coefficients in Labyrinth Seals. In Proceedings of the ASME 1987 International Gas Turbine Conference and Exhibition, Anaheim, CA, USA, 31 May–4 June 1987. ASME Paper 87-GT-188.
7. Waschka, W.; Wittig, S.; Kim, S. Influence of high rotational speeds on the heat transfer and discharge coefficients in labyrinth seals. *J. Turbomach.* **1992**, *114*, 462–468. [[CrossRef](#)]
8. Tipton, D.L.; Scott, T.E.; Vogel, R.E. *Labyrinth Seal Analysis*; ASME: New York, NY, USA, 1986; Volume III: Analytical and experimental development of a design model for labyrinth seals, AFWAL-TR-85-2103.
9. Chupp, R.E.; Holle, G.; Scott, T.E. *Labyrinth Seal Analysis*; ASME: New York, NY, USA, 1986; Volume IV: User's manual for the labyrinth seal design model, AFWAL-TR-85-2103.
10. Zimmermann, H.; Wolff, K.H. Air System Correlations, Part 1: Labyrinth Seals. In Proceedings of the ASME 1998 International Gas Turbine and Aeroengine Congress and Exhibition, Stockholm, Sweden, 2–5 June 1998. ASME Paper 98-GT-206.
11. Zimmermann, H.; Kammerer, A.; Wolff, K.H. Performance of Worn Labyrinth Seals. In Proceedings of the ASME 1994 International Gas Turbine and Aeroengine Congress and Exposition, The Hague, The Netherlands, 13–16 June 1994. Paper 94-GT-131.
12. Rhode, D.L.; Johnson, J.W.; Broussard, D.H. Flow Visualization and Leakage Measurements of Stepped Labyrinth Seal: Part 1—Annular Groove. In Proceedings of the ASME 1996 International Gas Turbine and Aeroengine Congress and Exposition, Birmingham, UK, 10–13 June 1996. ASME Paper 96-GT-136.
13. Schramm, V.; Willenborg, K.; Kim, S.; Wittig, S. Influence of a honeycomb facing on the flow through a stepped labyrinth seal. *J. Eng. Gas Turbines Power* **2000**, *124*, 140–146. [[CrossRef](#)]
14. Schramm, V.; Denecke, J.; Kim, S.; Wittig, S. Shape optimization of a labyrinth seal applying the simulated annealing method. *Int. J. Rotating Mach.* **2004**, *10*, 365–371. [[CrossRef](#)]
15. Willenborg, K.; Kim, S.; Wittig, S. Effects of Reynolds Number and Pressure Ratio on Leakage Loss and Heat Transfer in a Stepped Labyrinth Seal. In Proceedings of the ASME Turbo Expo 2001: Power for Land, Sea, and Air, New Orleans, LA, USA, 4–7 June 2001. ASME Paper 2001-GT-0123.
16. Doğu, Y.; Sertçakan, M.C.; Bahar, A.S.; Pişkin, A.; Arıcan, E.; Kocagül, M. CFD Investigation of Labyrinth Seal Leakage Performance Depending on Mushroom Shaped Tooth Wear. In Proceedings of the ASME Turbo Expo 2015: Power for Land, Sea, and Air, Montreal, QC, Canada, 15–19 June 2015. ASME Paper GT2015-43607.
17. Yan, X.; Dai, X.; Zhang, K.; Li, J.; He, K. Effect of teeth bending and mushrooming damages on leakage performance of a labyrinth seal. *J. Mech. Sci. Technol.* **2018**, *32*, 4697–4709. [[CrossRef](#)]
18. Yan, X.; Dai, X.; Zhang, K.; Li, J.; He, K. Influence of Hole-Pattern Stator on Leakage Performance of Labyrinth Seals. In Proceedings of the ASME Turbo Expo 2018: Power for Land, Sea, and Air, Oslo, Norway, 11–15 June 2018. ASME Paper GT2018-75349.
19. Kim, T.S.; Kang, Y.; Moon, H.K. Aerodynamic performance of double-sided labyrinth seals. In *Fluid Machinery and Fluid Mechanics*; Springer: Berlin/Heidelberg, Germany, 2009; pp. 377–382.
20. Kim, T.S.; Cha, K.S. Comparative analysis of the influence of labyrinth seal configuration on leakage behavior. *J. Mech. Sci. Technol.* **2009**, *23*, 2830–2838. [[CrossRef](#)]
21. Kim, T.S.; Kang, S.Y. Investigation of leakage characteristics of straight and stepped labyrinth seals. *Int. J. Fluid Mach. Syst.* **2010**, *3*, 253–259. [[CrossRef](#)]

22. Kang, Y.; Kim, T.S.; Kang, S.Y.; Moon, H.K. Aerodynamic Performance of Stepped Labyrinth Seal for Gas Turbine Applications. In Proceedings of the ASME Turbo Expo 2010: Power for Land, Sea, and Air, Glasgow, UK, 14–18 June 2010. ASME Paper GT2010-23256.
23. Zhang, L.; Zhu, H.R.; Liu, C.L.; Tong, F. Experimental and Numerical Investigation on Leakage Characteristic of Stepped Labyrinth Seal. In Proceedings of the ASME Turbo Expo 2016: Power for Land, Sea, and Air, Seoul, Korea, 13–17 June 2016. Paper GT2016-56743.
24. Vakili, A.D.; Meganathan, A.J.; Michaud, M.; Radhakrishnan, S. An Experimental and Numerical Study of Labyrinth Seal Flow. In Proceedings of the ASME Turbo Expo 2005: Power for Land, Sea, and Air, Reno, NV, USA, 6–9 June 2005. ASME Paper GT2005-68224.
25. Braun, E.; Dullenkopf, K.; Bauer, H.J. Optimization of Labyrinth seal Performance Combining Experimental, Numerical and Data Mining Methods. In Proceedings of the ASME Turbo Expo 2012: Power for Land, Sea, and Air, Copenhagen, Denmark, 11–15 June 2012. ASME Paper GT2012-68077.
26. Kline, S.J. The purposes of uncertainty analysis. *J. Fluids Eng. Trans.* **1985**, *107*, 153–160. [[CrossRef](#)]
27. ANSYS Inc. *ANSYS CFX 19.0*; ANSYS Inc.: Canonsburg, PA, USA, 2018.
28. ANSYS Inc. *ANSYS CFX-Solver Modeling Guide*; ANSYS Inc.: Canonsburg, PA, USA, 2011.
29. Menter, F.R. Two-equation eddy-viscosity turbulence models for engineering applications. *AIAA J.* **1994**, *32*, 1598–1605. [[CrossRef](#)]
30. Coughtrie, A.R.; Borman, D.J.; Sleigh, P.A. Effects of turbulence modelling on prediction of flow characteristics in a bench-scale anaerobic gas-lift digester. *Bioresour. Technol.* **2013**, *138*, 297–306. [[CrossRef](#)] [[PubMed](#)]

Publisher’s Note: MDPI stays neutral with regard to jurisdictional claims in published maps and institutional affiliations.



© 2020 by the authors. Licensee MDPI, Basel, Switzerland. This article is an open access article distributed under the terms and conditions of the Creative Commons Attribution (CC BY) license (<http://creativecommons.org/licenses/by/4.0/>).